Symmetry breaking and light-induced spin-state trapping in a mononuclear FeII complex with the two-step thermal conversion

Marylise Buron-Le Cointe, Nawell Ould-Moussa, E. Trzop, Alain Moréac, Gábor Molnár, Loïc Toupet, Azzedine Bousseksou, Jean-François Letard, Galina Matouzenko

Symmetry breaking and light-induced spin-state trapping in a mononuclear Fe^{II} complex with the two-step thermal conversion

M. Buron-Le Cointe,[1,*] N. Ould Moussa,[1,2] E. Trzop,[1] A. Moréac,[1] G. Molnar,[2] L. Toupet,[1] A. Bousseksou,[2] J. F. Létard,[3] and G. S. Matouzenko[4]

[1]*Institut de Physique de Rennes, Université de Rennes 1–CNRS, UMR 6251, Bât. 11A Campus de Beaulieu, 35042 Rennes, France*

[2]*Laboratoire de Chimie de Coordination, CNRS UPR-8241, Université de Toulouse, INP, UPS, 31077 Toulouse, France*

[3]*ICMCB, CNRS–Université Bordeaux, 87 Av. du Doc. A. Schweitzer, 33608 Pessac, France*

[4]*Laboratoire de Chimie, CNRS–Ecole Normale Supérieure de Lyon, UMR 5182, 46 allée d'Italie, 69364 Lyon Cédex 07, France*

(Received 7 September 2010; published 10 December 2010)

Crystallographic, magnetic, and Raman investigations of the mononuclear $[Fe^{II}(Hpy\text{-}DAPP)](BF_4)_2$ complex are presented. Its particular feature is a two-step thermal spin conversion in spite of a unique symmetry-independent iron site per unit cell. The plateau around 140 K is associated with a symmetry breaking visible by the appearance of weak $(0k0)$ k odd Bragg peaks. Symmetries of the high-temperature high-spin state and of the low-temperature low-spin state are both monoclinic $P2_1/c$, so that the symmetry breaking on the plateau is associated with a reentrant phase transition. It is discussed in relation with Ising-type microscopic models. At the plateau level, the two symmetry-independent molecules differ both by their spin state and the conformation (*chair* versus *twist-boat*) of one metallocycle. At low-temperature photoinduced phenomena have been investigated: a partial phototransformation [light-induced excited spin-state trapping (LIESST) effect] is observed under visible red irradiation. Raman spectroscopy shows that the molecular photoinduced state is the high-spin one. Nevertheless, as no macroscopic symmetry breaking is observed, the unique average cationic $[Fe^{II}(Hpy\text{-}DAPP)]$ state of the unit cell is intermediate between pure low-spin and high-spin states and presents a conformational disorder for one metallocycle. Reverse-LIESST has also been evidenced using near infrared excitation. Thus, the mononuclear $[Fe(Hpy\text{-}DAPP)](BF_4)_2$ compound offers the opportunity to discuss the interplay between spin conversion, molecular conformational change, and ordering processes.

DOI: 10.1103/PhysRevB.82.214106 PACS number(s): 61.50.Ks, 42.70.Gi, 75.30.Wx, 78.30.−j

I. INTRODUCTION

Thermal equilibrium and out-of-equilibrium light-induced spin-state conversions have been extensively studied during the three last decades,[1,2] in particular, since the discovery of the light-induced excited spin-state trapping (LIESST) effect in the spin crossover crystal $[Fe^{II}(ptz)_6](BF_4)_2$.[3] In the solid state, the spin conversion can be accompanied by weak or strong cooperative effects originating from intermolecular elastic interactions as the molecular size depends on the spin state.[4–8] Two major types of thermal spin-state switching have been observed and described: (a) one-step conversion with or without hysteresis accompanied in some cases by a crystallographic phase transition, (b) two-step conversion with continuous or discontinuous steps delimiting a plateau, which usually corresponds to approximately equal populations of high-spin (HS) and low-spin (LS) molecules. In this last case, the problem of the occurrence of a symmetry breaking on the plateau is posed. It could have been solved only recently in the case of $[Fe(2\text{-pic})_3]Cl_2.EtOH$ (Ref. 9) with the observation of a cell doubling on the plateau.[10,11] At variance with $[Fe(2\text{-pic})_3]Cl_2.EtOH$ previous structural investigations of the mononuclear $[Fe(Hpy\text{-}DAPP)](BF_4)_2$ complex, which also presents a two-step thermal spin conversion, had concluded to an isostructural spin-state switching with a monoclinic $P2_1/c$ symmetry at all temperatures.[12] The HS and the LS molecular states have been associated with a *chair* and a *twist-boat* conformation of one six-membered metallocycle, respectively (Fig. 1). The plateau had then been related to an unusual enhancement of the disorder in the $[FeN_6]$ coordination core associated with the appearance of this *twist-boat* conformation as the temperature decreases. It was the observation of conformational change associated with a spin conversion in the solid state. Moreover, in $[Fe(2\text{-pic})_3]Cl_2.EtOH$, there is contradictory information on the symmetry of the photoexcited state: whereas the average macroscopic photoinduced symmetry is the one of the HS state at thermal equilibrium,[11,13] Raman spectroscopy has evidenced a local symmetry breaking.[14,15] These results motivated us to reconsider the

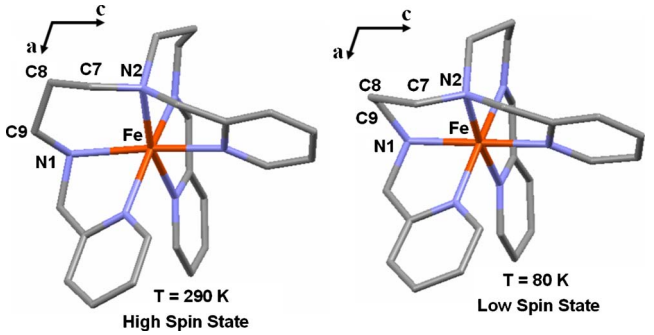

FIG. 1. (Color online) [Fe(Hpy-DAPP)] cation in the HS state (left) and in the LS state (right) in projection parallel to the **b** unit-cell axis. Directions of **a** and **c** unit-cell axis are indicated by arrows. The BF_4 anion and hydrogen atoms are omitted for clarity. The six-membered FeN1C9C8C7N2 metallocycle switches from a HS *chair* to a LS *twist-boat* conformation as observed in Ref. 12. Orientation of other cycles with respect to the Fe atoms also changes as illustrated here.

crystallographic study of the two-step spin crossover compound $[Fe^{II}(Hpy\text{-}DAPP)](BF_4)_2$ (Ref. 12) at thermal equilibrium and to undertake complementary experimental investigations both at thermal equilibrium and under light irradiation to obtain an overview. This paper presents and discusses experimental results obtained by x-ray diffraction, magnetic measurements, and also Raman spectroscopy. It is divided in three parts: the first one (Sec. III) presents new magnetic measurements at thermal equilibrium as well as the symmetry-breaking analysis on the thermal plateau and structural signatures of the spin conversion observed on the lattice parameters. The second part (Sec. IV) presents out-of-equilibrium phenomena evidenced after weak continuous light irradiation in the 630–660 nm range. Then the third part (Sec. V) is devoted to detailed structural analysis both at thermal equilibrium and under light irradiation and to discussion in relation with microscopic Ising-type model of two-step spin crossovers.

II. EXPERIMENTS

The mononuclear $[Fe(Hpy\text{-}DAPP)](BF_4)_2$ complex was obtained according to a procedure previously reported.[12] *Crystallographic measurements* at thermal equilibrium and under continuous light irradiation $\lambda=658$ nm from 4 to 10 mW cm^{-2} were performed on single crystals of typical sizes around $300\times200\times100$ μm^3. Data were collected on a four-circle Oxford diffraction Xcalibur 3 diffractometer (Mo $K\alpha$ radiation, $\lambda=0.71069$ Å) equipped with a two-dimensional Sapphire 3 charge-coupled device (CCD) detector. The single crystals were mounted in an Oxford Cryosystem nitrogen-flow cryostat for measurements down to 80 K, with a temperature stability of 0.1 K. The unit-cell parameters and the data reduction were obtained with CRYSALIS software from Oxford diffraction.[16] Structures were solved with SIR-97 (Ref. 17) and refined with SHELX.[18] Typical results of the structure refinements gave final $R1$ factor $0.04<R1<0.09$.[19]

Variable-temperature *Raman spectra* were collected in the 150–1700 cm^{-1} frequency range using a LabRAM-HR (Jobin Yvon) Raman spectrometer. A small single crystal of the compound $[Fe(Hpy\text{-}DAPP)](BF_4)_2$ was enclosed under nitrogen atmosphere on the cold finger of a THMS600 (Linkam) liquid nitrogen cryostat. The 632.818 nm line of a 15 mW He-Ne laser or the 785 nm line of a 70 mW laser diode was used as the excitation source. The exciting radiation was directed through a neutral density filter (optical densities 2 and 1 for 632.8 nm and 785 nm, respectively) to avoid sample heating problems and was focused on the sample via a $\times50$, 10.6 mm long working-distance objective. The scattered light was collected in backscattering configuration and the Rayleigh scattering was removed by means of a holographic notch/or dielectric edge filter.

The variable-temperature *magnetic-susceptibility measurements* were obtained on a thin layer of polycrystalline compound with a magnetic property measurement system (MPMS)-55 Quantum Design superconducting quantum interference device (SQUID) magnetometer with an operating field of 2 T within the temperature range of 10–300 K. The photomagnetic measurements were carried out using the light source of a Spectra Physics Series 2025 Kr^+ laser ($\lambda=647$ nm) coupled by an optical fiber to the cavity of the SQUID magnetometer. The laser light power at the sample was adjusted to 20 mW/cm^2.

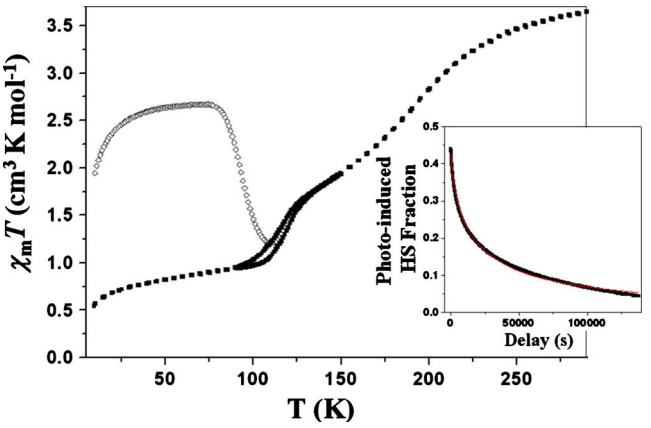

FIG. 2. (Color online) Temperature dependence of the $\chi_M T$ product. $\chi_M T$ follows the law $(\chi_M T) \sim \frac{1}{8}g^2[S(S+1)]$ where χ_M is the molar magnetic susceptibility, T the temperature, g the Landé factor ($g\approx2$), and S the molecular spin state. The closed circles show a thermal cycle (295 K–2 K–295 K) recorded in the dark, while the open circle symbols show the evolution of $\chi_M T$ in the dark when heating the sample from 10 to 130 K following light irradiation (647 nm) at 10 K under irradiation. (Insert) Relaxation of the metastable HS fraction observed at 90 K, i.e., slightly below T(LIESST). The experimental curve (black) is well fitted by a stretched exponential law, thus introducing a Gaussian width of the activation energy of 100 cm^{-1}.

III. PART I: THERMAL SPIN CONVERSION AND SYMMETRY-BREAKING ANALYSIS

The thermal dependence of the magnetic susceptibility of the $[Fe(Hpy\text{-}DAPP)](BF_4)_2$ complex was previously described.[12] The $\chi_M T$ product, where χ_M stands for the molar magnetic susceptibility, presents a two-step spin conversion with a plateau at around 140 K (Fig. 2). At this temperature approximately 50% of the molecules have changed their spin state. The low-temperature step is more abrupt than the first one centered around 190 K and presents a small thermal hysteresis of 3–4 K width. New measurements (Fig. 2) have been performed before investigating photoinduced phenomena. One can notice that in the present study, the thermal hysteresis is spread over a range of around 60 K (between $\chi_M T\approx0.925$ cm^3 mol^{-1} K at 85 K and $\chi_M T\approx1.88$ cm^3 mol^{-1} K at 145 K) whereas it appeared limited to about 25 K in the previous study (see Fig. 1 in Ref. 12). Such differences might be explained by the strong sensitivity of the sample to the cooling rate during the second step. The origin of the hysteresis is kinetic and was related tentatively to the slow conformational change in the ligand at low temperature. The Mössbauer experiments previously reported revealed that the residual HS fraction at low temperature strongly depends on the cooling rate. For example, a very slow cooling to 80 K at a rate of 0.1 K min^{-1} leads to the

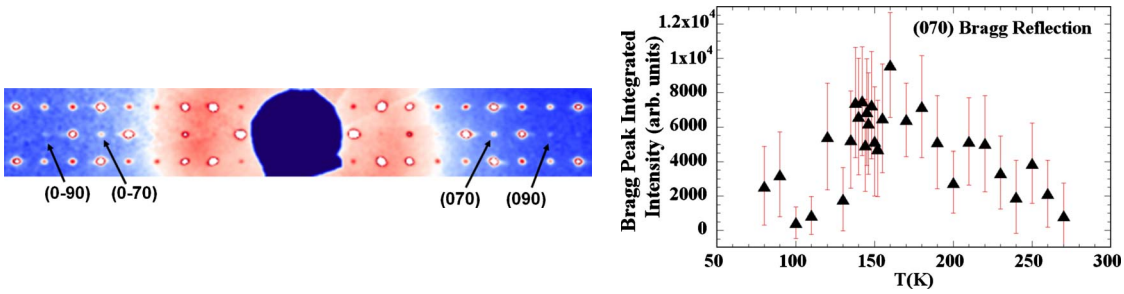

FIG. 3. (Color online) (Left) ($\mathbf{b}^*\mathbf{c}^*$) reciprocal plane observed on the plateau at 145 K. Weak ($0k0$) reflections with k odd are observed as indicated by arrows. (b^* and c^* axes are horizontal and vertical ones, respectively.) (Right) Integrated intensity of (070) Bragg reflections as a function of temperature, collected by omega scans. Intensities and sigma values are obtained with CRYSALIS software from Oxford diffraction (Ref. 16). The peaks do not significantly come out of the background at high and low temperatures.

residual HS fraction of 8% while a cooling rate of 50 K min^{-1} results in 32% trapped HS species.[12] In the present work, we observe that it is possible to obtain the LS phase quite rapidly by quenching the compound from room temperature to 108 K since the relaxation of the trapped HS state down to the stable LS phase is relatively quick at this temperature. At lower temperatures, a slow cooling down is necessary since the HS→LS conversion rate becomes then quite slow and such behavior is favorable to the observation of the LIESST effect. In both former and present studies the spin conversion is incomplete at low temperature with here a residual HS fraction of about 25% at 80 K ($\chi_M T \approx 0.9$ cm^3 mol^{-1} K) which decreases down to around 15% at 10 K ($\chi_M T \approx 0.56$ cm^3 mol^{-1} K).

The present structural investigations done with a new generation of CCD detector which considerably increases the signal/noise ratio for weak Bragg reflections clearly show that a symmetry breaking occurs on the plateau with the appearance of weak ($0k0$) k odd reflections (Fig. 3). These are the signature of the loss of the screw axis 2_1 parallel to the **b** crystallographic axis and simultaneously of the inversion symmetry on the plateau. The corresponding space group is then Pc with two independent molecules in the unit cell (Fig. 4). These additional Bragg peaks disappear again when temperature decreases so that the average symmetry is the same in the high-temperature HS phase and in the low-temperature LS one, i.e., $P2_1/c$. Thus, the present symmetry-breaking analysis reveals a so-called reentrant phase transition associated with the spin conversion and a symmetry breaking occurring on the plateau. Besides we could observe clear signatures of the two-step spin conversion in the evolution of the unit-cell volume and parameters, as a function of temperature (Fig. 5). Whereas the first step of the spin conversion is not sensitive to the cooling rate, on the contrary the second step (and more specifically the low-temperature area, i.e., below 110–100 K) is strongly influenced by the sample history and the cooling rate. The curves here presented were obtained for the first cooling of not-twinned crystals with a cooling rate lower than 2 K min^{-1}. The temperature was stabilized by step of 5 K for data collection. A second slow cooling without any stabilized step in temperature could never lead to the same values for the lattice parameters even with a slow cooling rate of 0.5 K min^{-1}. Thus values obtained for the lattice parameter **a** as an example, varies from 12.27 Å (Fig. 5) up to 12.61 Å without however affecting the observed average symmetry $P2_1/c$. Such a strong sensitivity of the sample to the cooling procedure was already observed on previous Mössbauer measurements[12] as discussed here above: whereas the plateau always corresponds to an equal proportion of HS and LS molecules, the spin conversion ratio below this plateau at 80 K significantly decreases with the increase in the cooling rate.

The present symmetry-breaking analysis is a new illustration of the importance of careful crystallographic studies before concluding to the existence or not of a reentrant phase transition associated with the spin conversion. As an example, the origin of the two-step conversion in $[Fe(2\text{-pic})_3]Cl_2.EtOH$ (Ref. 9) has been solved only quite recently:[10,11] the alternation of planes with HS or LS molecules manifests itself by the appearance of numerous new Bragg reflections indexed $(\frac{h}{2},k,\ell)$ in the high- or low-temperature space group due to a doubling of the unit-cell axis $\vec{a}$. The case of $[Fe(Hpy\text{-}DAPP)](BF_4)_2$ here presented is more delicate because the symmetry breaking is associated with the appearance of a few weak Bragg reflections indexed ($0k0$) with k odd. Such Bragg reflections are sensitive to the atomic displacements parallel to the cell axis **b** and their

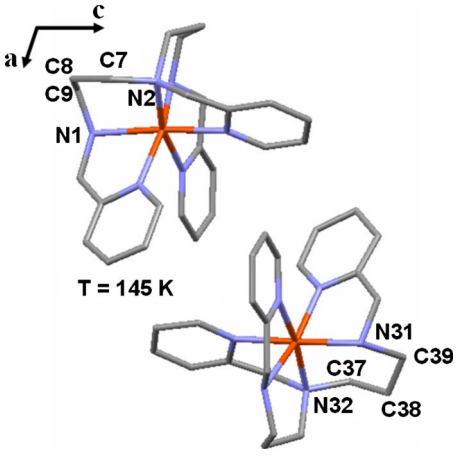

FIG. 4. (Color online) Projection parallel to the **b** unit-cell axis of the two independent molecules observed on the plateau due to the symmetry breaking. Directions of **a** and **c** unit-cell axis are indicated by arrows.

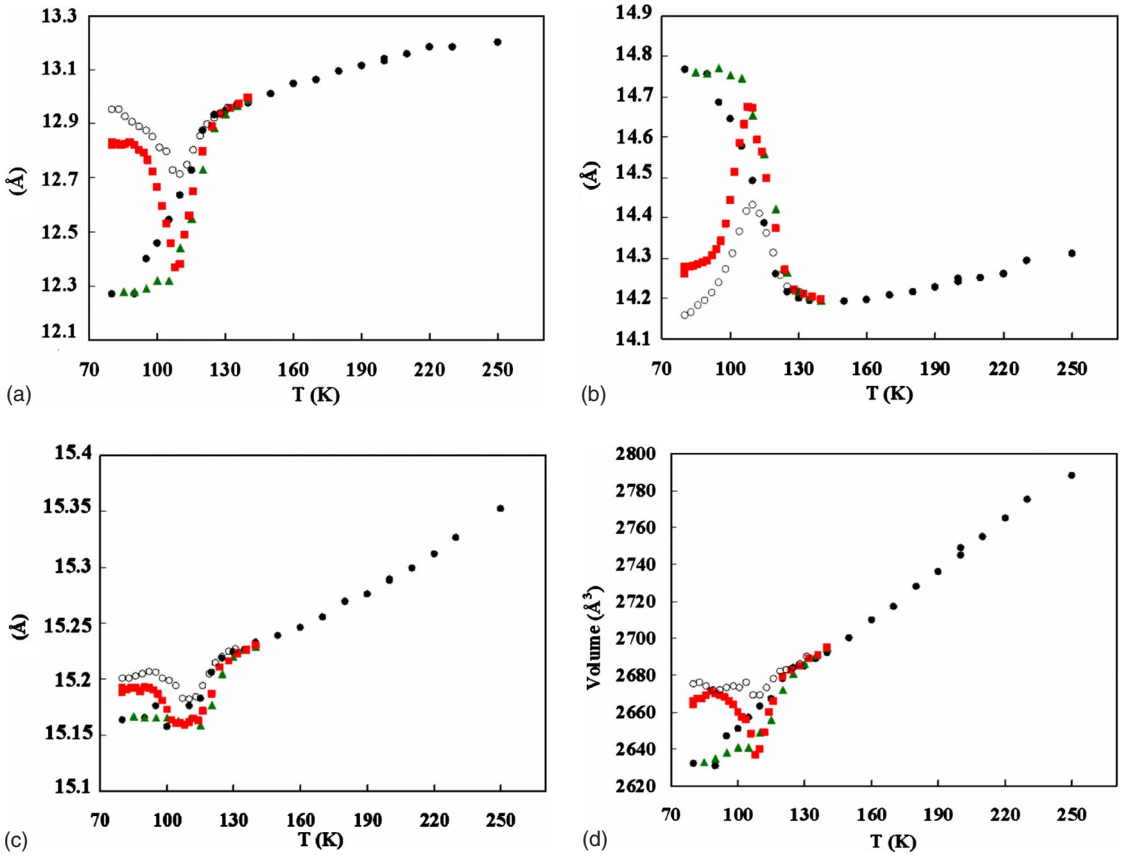

FIG. 5. (Color online) Evolution of the unit-cell volume and parameters, as a function of temperature. Black circle and green triangle points represent the cooling and the heating measurements, respectively. Open points are data collected after a thermal quenching of the sample at 80 K and red square points are data collected after continuous irradiation ($\lambda = 658$ nm, 4 mW) made at 80 K.

weakness is then directly related to very little atomic displacements in this direction.

Two-step spin conversions have already been observed in some other mononuclear spin-crossover compounds presenting two independent iron sites per unit cell,[20–25] and can be described by a microscopic two-sublattice Ising-type model combining intrasublattice J_A and J_B ferromagnetic interactions with intersublattice J_{AB} antiferromagnetic ones[26–29] or from a phenomenological point of view by a Landau-type approach.[30] In such a situation a symmetry breaking is possible but not necessary. The $[Fe(Hpy\text{-}DAPP)](BF_4)_2$ system is different in the sense that, like $[Fe(2\text{-}pic)_3]Cl_2.EtOH$, the unit cell contains only one symmetry-independent iron site in the $P2_1/c$ space group. The nature of the symmetry breaking is then essential to show there are two kinds of molecular states per unit cell at the plateau level. The model is discussed in relation with detailed crystallographic analysis in part III.

IV. PART II: INVESTIGATIONS OF PHOTOINDUCED PHENOMENA

Photoinduced phenomena were observed through magnetic-susceptibility measurements by shining the sample with a red laser ($\lambda = 647$ nm, 20 mW/cm^2) after reaching the temperature of 10 K. After about 14 h of irradiation, the $\chi_M T$ product changes from the initial value of 0.85 cm^3 mol^{-1} K up to 1.94 cm^3 mol^{-1} K and saturates (Fig. 2). Then, the compound was heated in the dark to 130 K at the rate of 0.3 K min^{-1}, in order to follow the evolution of the metastable photoinduced state. The signal first increases slightly in the vicinity of 10–30 K due to the zero-field splitting of the photoinduced metastable HS state. Then, it remains almost constant between 30 and 80 K. In this temperature range, apparently, the relaxation process is much slower than the time scale of the magnetic measurement. The comparison with the measured $\chi_M T$ product for the pure HS state at room temperature ($\chi_M T = 3.62$ cm^3 mol^{-1} K) indicates that the observed LIESST effect on the $[Fe(Hpy\text{-}DAPP)](BF_4)_2$ compound is somewhat partial (65%). Finally, the $\chi_M T$ product drops in the range of 80–100 K. The T(LIESST) temperature,[31,32] defined as the minimum of the derivative curve of the Fig. 2 recorded during the thermally induced relaxation is estimated to approximately 93 K. Inset of Fig. 2 shows the relaxation curve of the metastable photoinduced state at 90 K. Despite the occurrence here of a thermal hysteresis in the second step of the transformation at thermal equilibrium, the observed decay curve does not present a sigmoidal shape characteristic of cooperative effects.[1,33] The most striking feature of this relaxation curve is the clear deviation from single exponential and a marked stretched exponential behavior with a fast component at earlier times and a long decay process at infinite

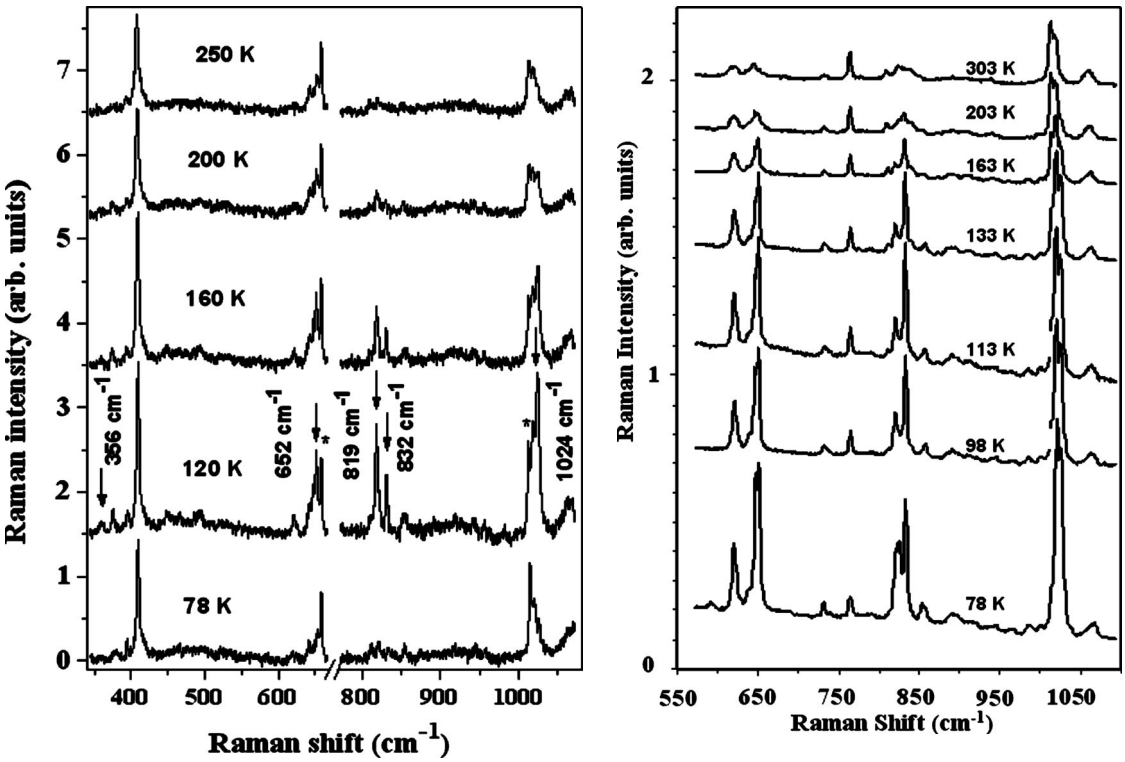

FIG. 6. Representative Raman spectra of $[Fe(Hpy\text{-}DAPP)](BF_4)_2$ complex at different temperatures: measurements performed at 632.8 (A, left) nm and 785 nm (B, right).

times. Such stretched exponential behaviors have already been mentioned in disordered systems, like an iron (II) spin crossover complex dispersed into a polymer matrix[34] as well as in single crystal like $[Fe(ptz)_6](BF_4)_2$ for the relaxation of the supercooled HS phase ($R\bar{3}$ symmetry) toward the low-temperature LS disordered structure.[35,36] This reveals the inhomogeneous character of the sample. For fitting the curves, a distribution of relaxation rates at a given temperature with a Gaussian distribution of the activation energy has been introduced.[31] Such kind of relaxation in $[Fe(Hpy\text{-}DAPP)](BF_4)_2$ is however less surprising after the study of the photoinduced phase: the phototransformation occurs without any symmetry breaking, i.e., continuously without any phase transition; the photoinduced phase is very similar to the quenched one with an average symmetry $P2_1/c$ and a disorder on one metallocycle of the [Fe(Hpy-DAPP)] cation (see part III).

The $[Fe(Hpy\text{-}DAPP)](BF_4)_2$ complex was also studied by Raman spectroscopy excited at 632.8 nm and at 785 nm (Fig. 6). One can immediately notice that no broadening of internal and external Raman modes is visible in the plateau region, so that there is no signature of disorder in perfect agreement with the reentrant phase transition associated with the two-step spin conversion (see part I).

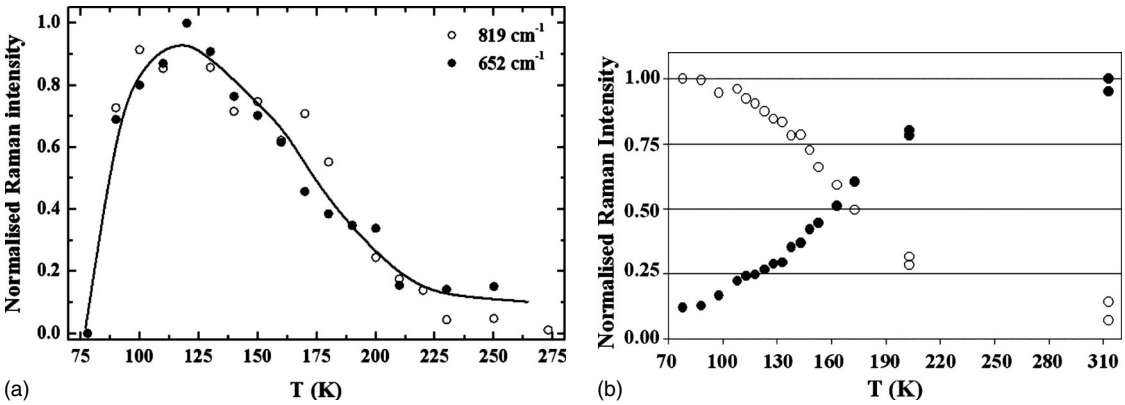

FIG. 7. (a) Temperature dependence of the intensities of the 652 and 819 cm^{-1} Raman modes (normalized to the intensity of the 658 cm^{-1} mode) in $[Fe(Hpy\text{-}DAPP)](BF_4)_2$ with the 632.8 nm excitation. (b) Temperature dependence of the intensities of the 1015 cm^{-1} (●) and 1024 cm^{-1} (○) Raman modes (normalized to the intensity of the 1020 cm^{-1} mode) in $[Fe(Hpy\text{-}DAPP)](BF_4)_2$ with the 785 nm excitation.

We have experimentally observed at least five Raman modes (647, 652, 819, 832, 1024 cm^{-1}) reversibly appearing/disappearing as a function of the temperature (Figs. 6 and 7). These are very likely sensitive to the conformational change from *chair* to *twist-boat* of the FeN1C9C8C7N2 metallocycle (see part III). This observation was done under 785 nm excitation as well as under 632.8 nm excitation except at 78 K, i.e., below T(LIESST)=93 K. In view of the photoinduced phenomena observed by pumping at 647 nm or 658 nm, the 632.8 nm wavelength used in Raman does not allow to observe the pure LS state since at low temperature it acts as a pump for the crystal, whereas the 785 nm wavelength does (Fig. 6). The 78 K Raman spectrum looks then very similar to the high-temperature one without any broadening of any Raman modes when pumping at 632.8 nm. This suggests a complete photoinduced transformation inside the "volume" probed by Raman spectroscopy, i.e., essentially the sample surface. This Raman study clearly demonstrates the HS nature of the photoinduced molecular state. The Raman spectrum of the pure LS phase can be observed only when exciting at 785 nm.

Besides, different attempts to obtain a photoinduced Raman spectrum at 785 nm by using an external continuous 658 nm diode (the one used for photoinduced diffraction measurements) as a pump were unsuccessful. We then verify that this might be caused by a pump (658 nm) and dump (785 nm) effect by following the time evolution of unit-cell parameters under successive light irradiation at 658 and 800 nm (Fig. 8). A reverse-LIESST effect at 800 nm was thus unambiguously evidenced.

Structural aspects of both the quenched HS state and the photoinduced one have been followed by x-ray diffraction measurements. Complete data collections performed at 80 K in both cases revealed an average monoclinic symmetry with the space group $P2_1/c$ (Fig. 9) and are discussed in details in part III. Here we present the temperature evolution of the unit-cell parameters after the quenching (open points, Fig. 5) and also after the observation of the photoinduced phenomenon (red square points, Fig. 5). One can notice that the unit-cell volume and parameters are slightly lower in the photoinduced state than in the quenched one. But evidently, the two cases differ mainly by the evolution when heating the crystal: on one hand, after the quenching the lattice parameters curves join those observed in the cooling mode around 110 K (i.e., slightly above T(LIESST) where the relaxation processes down to the thermal equilibrium state are very fast). On the other hand, after the phototransformation at 80 K and again around 110 K the lattice parameters join the points measured at thermal equilibrium in the heating mode, i.e., follow the hysteresis curve. These thermal evolutions show that, as already observed,[2] the first-order transition is suppressed by the quenching.

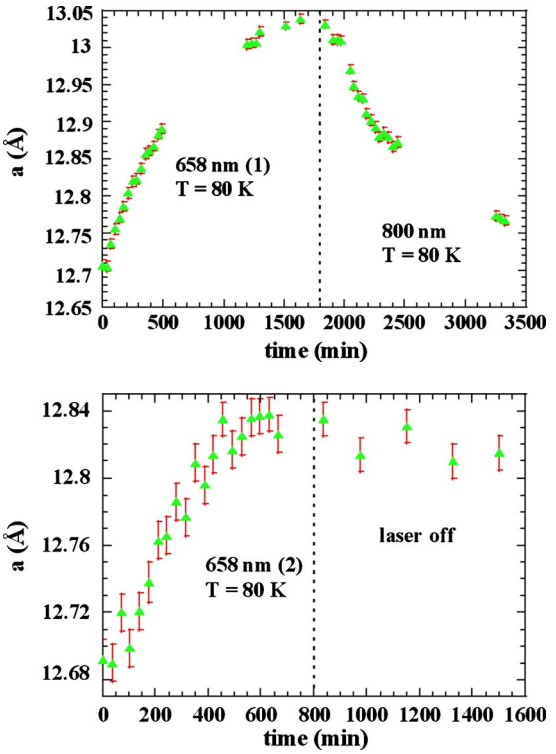

FIG. 8. (Color online) LIESST (excitation at 658 nm) and reverse-LIESST (excitation at 800 nm) observed on the time evolution of **a** unit-cell parameter at 80 K. Two thermal cycles have been registered: a first photoexcitation at 658 nm labeled (1) followed by an irradiation at 800 nm (top), a second photoexcitation at 658 nm labeled (2) followed by measurements in the dark (bottom). The crystal quality has sensitively decreased after the first thermal cycle as visible on errors bars.

V. PART III: DETAILED CRYSTALLOGRAPHIC ANALYSIS AND DISCUSSION

We present here in details our crystallographic data[19] and discuss the spin-state switching both from the molecular point of view and from intermolecular interactions. Structure refined in the high-temperature HS state, from 290 K down to 190 K in the space group $P2_1/c$ are very similar to the one previously discussed at 298 K,[12] except that the quite high atomic displacement parameter of N3 could not have been solved by a disorder between two atomic positions (Table I). The fluorine atoms of the two BF_4 counter ions are largely disordered and the average structures are solved with a 0.5:0.5 occupancy ratio of the two positions for each fluorine atom. There is only one symmetry independent molecule in the monoclinic unit cell. The average Fe-N bond length of 2.206(3) Å and a distortion parameter Σ of 89(2)° at 290 K

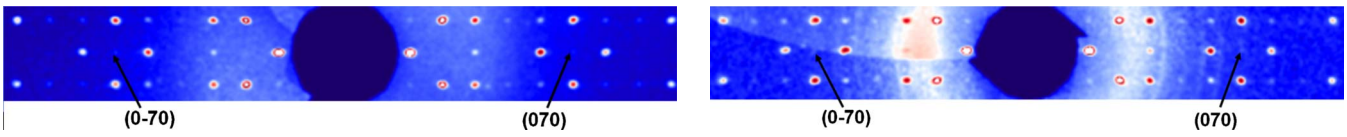

FIG. 9. (Color online) ($\mathbf{b}^*\mathbf{c}^*$) reciprocal plane observed at 80 K after quenching (left) and after light irradiation (λ=658 nm, 4 mW) (right). No ($0k0$) reflections with k odd are observed as indicated by arrows so the average symmetry is $P2_1/c$, i.e., the space group observed at high temperature. (b^* and c^* axis are horizontal and vertical ones, respectively.)

TABLE I. Equivalent isotropic thermal motion parameter, U_{eq} ($Å^2$), of two atoms labeled N3 and C9 in the [Fe(Hpy-DAPP)] cation as a function of temperature.

Temperature (K)	290	270	220	190	160	160 (disordered)	145	80	80, thermal quenching	80, 658 nm
Atom C9	0.097(2)	0.092(2)	0.098(3)	0.182(5)	0.313(10)	C9A: 0.064(7) C9B: 0.052(4)	C9: 0.077(3) C39: 0.049(2)	0.085(3)	C9A: 0.062(5) C9B: 0.034(4)	C9A: 0.052(4) C9B: 0.051(5)
Atom N3	0.148(3)	0.150(3)	0.158(5)	0.141(3)	0.142(3)	0.141(3)	N3: 0.044(1) N33: 0.044(1)	0.118(4)	0.129(4)	0.124(4)

(Table II) in the first coordination sphere of $Fe^{(II)}$ are characteristic of the HS molecular state.[37,38] This HS state is also easily recognizable with the *chair* conformation of the FeN1C9C8C7N2 metallocycle (Fig. 2 left). From the intermolecular point of view, it is important to notice both the shortest Fe…Fe distances gathered in Table III as well as close intermolecular contacts (distances shorter than the sum of van der Waals radii) mainly between the fluorine atoms of BF_4 anions and hydrogen or carbon atoms of the [Fe(Hpy-DAPP)] cation.[19] By lowering temperature down to the plateau, additional short contacts appear and the atomic displacement parameter of C9 increases significantly (Table I), so that at 160 K, two distinct positions can be clearly distinguished for this atom when solving the structure in the $P2_1/c$ geometry. Structure refinement in *Pc* space group [which is the good one in view of the symmetry-breaking analysis (Fig. 3)], lead to several negative atomic displacements parameters, thus evidencing strong correlations between atomic positions of the two molecules in the *Pc* unit cell. In other words, the loss of inversion symmetry consecutive to the $P2_1/c$ to *Pc* symmetry change mainly induce a geometry change in the FeN1C9C8C7N2 metallocycle but a pseudoinversion symmetry remains between other parts of the [Fe(Hpy-DAPP)] cation. As a consequence, the structure at 160 K has been refined in the space group $P2_1/c$ with the C9 atom disordered between two atomic positions labeled C9A and C9B.[19]

At 145 K however, refinement in the *Pc* space group works well and confirms that the two symmetry-independent molecules of the unit cell differ mainly by two different conformations of the FeN1C9C8C7N2 metallocycle (Fig. 4). The one labeled Fe1N1C9C8C7N2 has a *chair* conformation and the molecule has the longest average Fe-N bond length (Table II). It is closer to the molecular HS state than the second molecule. This latter presents a *twist-boat* conformation of the metallocycle now numbered Fe2N31C39C38C37N32. According to the average Fe-N bond length and Σ distortion, its spin state is intermediate between HS and LS. All atomic displacements parameters of the [Fe(Hpy-DAPP)] cation appear as standard ones for 145 K, even if those concerning the cycle here above mentioned (N1, C7, C8 and N31, C37, C38) appear now as being more anisotropic than at high temperature. A disorder remains on the BF_4 counter ions and only one among the four independent ones of the unit cell can be modeled with one position for one fluorine atom. For the three other molecules, the fluorine atoms are disordered between five positions whose occupancy ratio varies from 0.3 to 1. From the intermolecular point of view, the symmetry breaking leads to the doubling of different Fe…Fe distance values and it is interesting to notice that molecules in different spin states are closer to each other than HS or LS molecules (Table III). Moreover, as expected with the thermal lattice contraction, the number of intermolecular distances shorter than the sum of van der Waals radii has increased. The C9 and the C39 carbon atoms involved in the *chair* and *twist-boat* conformations of one cycle of the [Fe(Hpy-DAPP)] cation (Fig. 4) are now critically close not only to fluorine atoms but also to boron atoms of the BF_4 counter ions (Table IV). Thus we evidence that the *chair* to *twist-boat* conformational change in one metal-

TABLE II. Average bonding Fe-N lengths (Å) (left); distortion of the FeN_6 octahedron measured from the Σ parameter (Refs. 37 and 38), which is the sum of the 12 cis ϕ angles in the coordination sphere: $\Sigma = \Sigma_{i=1}^{12} |90 - \varphi_i|$ (right), as a function of temperature.

Temperature (K)	Average Fe-N bond length (Å)		Σ distortion parameter (deg)	
290	2.206(3)		89(2)	
270	2.206(3)		88(2)	
220	2.183(5)		83.4(2)	
190	2.156(4)		77.8(2)	
160	2.130(4)		69.9(2)	
145	2.152(6)	2.102(7)	87(3)	74(3)
80	2.050(6)		55(3)	
80, thermal quenching	2.095(6)		65(3)	
80, 658 nm	2.096(6)		65(3)	

TABLE III. Fe…Fe intermolecular shortest distances (Å) as a function of temperature.

Temperature (K)	Fe…Fe distances (Å)
290	7.831 10.150 10.304
270	7.815 10.154 10.302
220	7.759 10.104 10.259
190	7.726 10.113 10.271
160	7.676 10.077 10.253
145	HS-LS distances 7.634 9.611 9.289 9.800 HS-HS LS-LS 10.731 10.076
80	7.507 10.212 10.754
80, thermal quenching	7.569 10.078 10.186
80, 658 nm	7.574 10.105 10.191

locycle of the [Fe(Hpy-DAPP)] cation is directly related to steric constraints due to the closeness of BF_4 anions. These constraints are at the origin of the symmetry breaking observed on the plateau during the thermal spin-state change.

At 80 K, we solved the structure (space group $P2_1/c$, see part I symmetry-breaking analysis) with three different data collections for which lattice parameters differ due to the very high sensitivity of the hysteresis to the cooling process or to the sample history (see also part I). However, the average molecular structure (Fig. 2 right) does not depend on the values of lattice parameters and the *twist-boat* conformation of the metallocycle labeled FeN1C9C8C7N2 is always ob-

TABLE IV. Intermolecular contacts (in angstrom) between BF_4 and [Fe(Hpy-DAPP)] cation involving nonhydrogen atoms. An asterisk * marks the distances shorter than the sum of van der Waals radii. These are, respectively: C…F 3.17 Å N…F 3.02 Å N…B 3.55 Å C….B 3.70 Å Let remark that C…F distance values are indicative ones in view of the large atomic displacements parameters of fluorine atoms especially at high temperatures. (C39: HS state C9: LS state C9A: LS state, C9B: HS state.)

Temperature (K)	290	270	220	190	160	145	80	80, thermal quenching	80, 658 nm
C1…fluorine		3.168*	3.128*						
C3…fluorine		3.148*	3.078*	3.128*	3.134*	C33…F 3.100*	3.144*	3.107*	3.112
C4…fluorine		3.168*							3.168
C9…fluorine	*3.642* *3.837*	*3.648* *3.857*	*3.551* *3.732* *3.806*	*3.497* *3.528*	C9B…F: 3.010* C9A…F: 2.843* 3.064*	C39…F: 2.900* C9…F: 2.743*	3.113*	C9B…F: 2.812* 3.095* C9A…F: 2.918* 3.124*	C9B…F: 3.045* 2.860* C9A…F: 3.147* 2.977*
C17…fluorine						C47…F: 3.116*	3.117*; 3.144*		
C18…fluorine							2.674*	2.995*	2.993*
C19…fluorine	3.084*; 3.108*; 3.133*	3.072*; 3.100*	3.137*; 3.028*	3.151*	2.991* 3.133*	3.146* C49…F 3.006*	3.066*	3.000* 3.161*	2.998*
C22…fluorine	3.086*								
C21… fluorine			3.133*	3.125*		C51…F: 3.136*			
C23… fluorine			3.125*	3.159*		C53…F: 3.145*			
B1…C9	4.172	4.178	4.223	4.049	B1…C9A: 3.420*	B1…C39: 3.549*	3.541*	B1…C9A: 3.475*	B1…C9A: 3.481*
B1…C19	3.812	3.793	3.691*	3.776	3.760		3.803	3.786	3.785
B2…C9	3.906	3.886			B2…C9B: 3.661*	3.458*		B2…C9B: 3.491*	B2…C9B: 3.521*
B1…N1	3.544*	3.520*	3.552*	3.452*	3.476*		3.412*	3.442*	3.422*
B2…N3						3.545*			
B2…N1						3.470*			
B4…N31						3.504*			
N1…fluorine	2.938*	2.927*	2.916*	2.987*			2.997*		

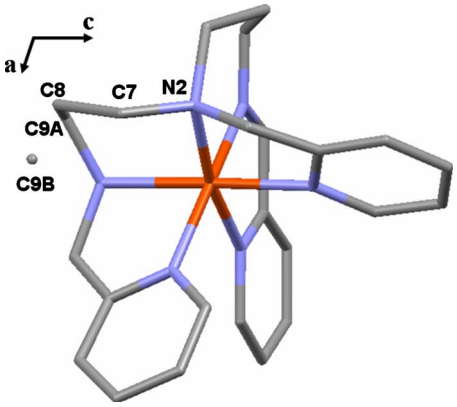

FIG. 10. (Color online) Average molecular state refined after data collected at 80 K, either after a thermal quenching or after light irradiation (λ=658 nm, 4 mW). In each case, the average atomic position of C9 is disordered with an occupancy ratio around 0.5:0.5 between C9A and C9B positions, corresponding to the LS and to the HS states, respectively. Projection is done parallel to the **b** unit-cell axis and directions of **a** and **c** unit-cell axis are indicated by arrows.

served with no significant differences in the average geometry of the first coordination sphere around Iron atom. By considering that the average Fe-N variation is 0.2 Å for iron(II) compounds[1,2] between HS and LS states, the value found here at 80 K, $\langle$Fe-N$\rangle \approx 2.050(6)$ Å is quite high. However it is not surprising in view of the kinetics effects already discussed in part I and only means that the average molecular state here obtained at 80 K is not the pure LS one. In spite of the low temperature value of 80 K, a disorder still remains on the two BF_4 counter ions: two fluorine atoms remain disordered between two positions on the first anion as well as one on the second anion, always with an occupancy ratio 0.7:0.3. As observed in the HS state, the atoms presenting the highest anisotropic thermal motion are N3 and its neighbors C17, C18, and C19. Concerning the intermolecular interactions, in addition to the short distances between fluorine of BF_4 and hydrogen of the [Fe(Hpy-DAPP)] cation, van der Waals contacts involve now also boron atoms of BF_4 with carbon and nitrogen atoms of the neighboring molecule [$C9\ldots B1$:3.541 Å *and* $N1\ldots B1$:3.412 Å (see Table IV)]. Besides, if the Fe…Fe distance between first neighboring molecules has still decreased at 80 K in comparison to highest temperatures, the distances between the second and third neighboring molecules increase significantly (Table III).

The refinement of the data collections registered at 80 K, but under different experimental conditions [LS state (Fig. 1 right), discussed in the former paragraph, quenched one, state obtained after irradiation at 658 nm] leads to different characteristic even if the average symmetry is $P2_1/c$ in each case (Fig. 10). Indeed, the average molecular spin state, either after the quenching or light irradiation, appears as an intermediate one (Fig. 10) between the HS and the LS ones (Fig. 1): a very large atomic displacement parameter appears for C9 which can be solved by refining two atomic positions C9A and C9B and their occupancy ratio is found to be close to 0.5:0.5 in both cases.[19] Thus, the thermal quenching does not lead to the quenching of the HS molecular state as observed in many one-step spin crossover systems, but to the quenching of a disordered mixed state with the HS and LS molecules in equal proportion. In other words, the quenching has stopped the ordering of HS and LS molecules which occurs at the plateau level during a standard cooling. On the other hand, the photoirradiation does never succeed in transforming the whole crystal: all our attempts lead to values between 0.4 and 0.55 for the HS molecular state. Such a partial phototransformation obtained through the crystallographic analysis has to be compared with the conversion shown by Raman investigations (Figs. 6 and 7) and to the 65% conversion obtained with photomagnetic experiments (Fig. 2). It may be related to a small penetration length of 647 nm light, as suggested by the dark green color of the sample and the strong absorption deduced from the Raman experimental conditions at this wavelength (see part II). If so, the structural refinement in the disordered $P2_1/c$ space group could be seen as resulting from the superposition of phototransformed regions of $P2_1/c$ symmetry with a *chair* conformation of the Fe1N1C9C8C7N2 metallocycle and nontransformed regions of $P2_1/c$ symmetry with a *twist-boat* conformation of the same metallocycle. Anyway, from the average point of view, thermal quenching and photoinduced states look then very similar and this is also true when looking at the intermolecular distances (Table III, Fe…Fe distances). Moreover, in the two cases, van der Waals interactions become stronger than for the LS state at thermal equilibrium with shorter intermolecular distances for boron-carbon but slightly weaker for boron-nitrogen distances (see Table IV). Notice that the absence of symmetry breaking and average disordered state under light irradiation is consistent with the one-step stretched exponential behavior which is observed during the relaxation in photomagnetic measurements (see part II).

As mentioned in part I, Ising-like microscopic models describing a two-step spin conversion in mononuclear spin-crossover compounds, combine two intrasublattice ferromagnetic-like interactions, J_A and J_B (J_A and $J_B>0$), with intersublattice antiferromagnetic-like one, J_{AB} (Refs. 26–29) ($J_{AB}<0$), whose role is to stabilize HS…LS pairs. The Hamiltonian is then

$$H = -J_A \sum_{\langle i,j \rangle} s_i^A s_j^A - J_B \sum_{\langle i,j \rangle} s_i^B s_j^B - J_{AB} \sum_{\langle i,j \rangle} s_i^A s_j^B - h_A \sum_i s_i^A - h_B \sum_i s_i^B,$$

where the fictitious spin states $S=-1,+1$ are associated with the LS and HS molecular states, respectively, i and j indices denote different sites. The two field terms, h_A and h_B, depend on the site energy difference Δ between HS and LS states and also on the degeneracy ratio g describing the entropy change between the two states,

$$h = -\frac{1}{2}(\Delta - k_B T \ln g) \quad \text{where} \quad g = \frac{g_{\mathrm{HS}}}{g_{\mathrm{LS}}}.$$

The degeneracy ratio stems from an electronic contribution originating from the spin multiplicity with possible orbital degeneracy and a molecular contribution due to the change

in vibrational frequencies between the HS and LS states.[39]

In the case of $[Fe(Hpy\text{-}DAPP)](BF_4)_2$ complex, it is reasonable to consider the particular case $J_A=J_B=J$ (A and B molecules are equivalent by symmetry at all temperatures except on the plateau) and then a two-step spin conversion can be explained only with the occurrence of a symmetry breaking ($J_{AB}\neq 0$) as experimentally observed at the plateau level. The Hamiltonian can then be treated in a mean-field approach and it is then shown that the plateau is bordered by a gradual spin conversion at high temperatures (here second-order structural transition due to the $P2_1/c \rightarrow Pc$ symmetry change discussed in part I) and a sharp first-order transition at low temperatures in the case where J is slightly larger than J_{AB}.[28] Our crystallographic analysis shows to a satisfactory extent that, at the plateau level, the HS…LS distances are shorter than the HS…HS or LS…LS ones (Table III) by comparison of the Fe…Fe intermolecular distances. Moreover, as our crystallographic analysis also shows that the two kinds of molecules coexisting in the unit cell on the plateau are both intermediate between pure HS and LS ones, it may be useful to complete the above Hamiltonian, in particular, with terms modeling conformational changes in ligand. A recent tentative which concerns the coupling between spin conversion and solvent disorder[40] might be an interesting starting point. Indeed, if in the crystals of $[Fe(Hpy\text{-}DAPP)](BF_4)_2$ complex there are no solvent molecules, a disorder is observed on BF_4 counter anions down to 80 K and the conformational change in the ligand is directly related to very short contacts between the metallocycle of [Fe(Hpy-DAPP)] and these anions.

To our knowledge, the $[Fe(Hpy\text{-}DAPP)](BF_4)_2$ is—*after the well-known example of* $[Fe(2\text{-}pic)_3]Cl_2.EtOH$—a second example of iron (II) mononuclear complex (one symmetry independent iron site per unit cell) presenting a two-step spin conversion. Three other examples have been published recently. In $[Fe(bapbpy)(NCS)_2]$,[41] the compound presents a (HS-LS-LS) long-range-ordered intermediate phase characterized by the appearance of surstructure Bragg peaks along $\frac{1}{3}\boldsymbol{c}^*$ and in a second one, a (HS-LS) long range order is visible by the appearance of structure Bragg peaks along $\frac{1}{2}\boldsymbol{c}^*$.[42] In the third case, the complex presents a thermal 50 K plateau associated with a random distribution of 50% HS and 50% LS sites[43] since no symmetry breaking has been evidenced up to now. At low temperature, after the photoinduced HS state trapping the observed relaxation is a two-step process. In view of these different behaviors observed on mononuclear iron (II) complexes further studies are necessary before having a complete understanding of the main physical parameters at the origin of the symmetry breaking and its necessity or not in the two-step spin-state change. It will be also of great interest to investigate the effect of pressure on the $[Fe(Hpy\text{-}DAPP)](BF_4)_2$ compound: a phenomenological Landau-type approach including symmetry consideration suggests the disappearance of the intermediate phase (i.e., the plateau) at high pressure.[30] In $[Fe(bapbpy)(NCS)_2]$,[44] the suppression of the (HS-LS-LS) $\rightarrow$ LS transition (second step) under pressure has been observed recently but then the symmetry breaking on the plateau was not associated with a reentrant phase transition at variance with $[Fe(Hpy\text{-}DAPP)](BF_4)_2$ and $[Fe(2\text{-}pic)_3]Cl_2.EtOH$ compounds.

VI. CONCLUSION

The thermal two-step spin conversion in the $[Fe(Hpy\text{-}DAPP)](BF_4)_2$ complex is associated with a reentrant phase transition (monoclinic symmetry $P2_1/c \rightarrow Pc \rightarrow P2_1/c$) and a symmetry breaking occurring on the plateau visible by the appearance of weak ($0k0$) *k odd* Bragg reflections. $[Fe(Hpy\text{-}DAPP)](BF_4)_2$ is thus the first complex presenting a symmetry breaking at the plateau level without any cell multiplication but related to the only loss of a symmetry element (screw axis 2_1). The spin conversion is also associated with a change in conformation of one metallocycle in relation with strong steric effects visible by close intermolecular contacts, in particular, between the [Fe(Hpy-DAPP)] cations and adjacent BF_4 anions. The plateau observed during the thermal spin conversion is directly related to this change in conformation and the two molecular spin states in the *Pc* unit cell are intermediate between pure HS and LS ones. After red light irradiation, a photoconversion toward a HS out-of-equilibrium state is observed. At the molecular level, this photoinduced state is the HS one as clearly visible on the Raman spectra. With both magnetic and crystallographic measurements only a partial conversion has been observed. X-ray analysis show that the average symmetry is similar to the one of the quenched state: the phototransformation occurs without any symmetry breaking (no phase transition). In a consistent way, the relaxation process does not present any self-accelerated character (cooperative effects) which would be taken into account by a sigmoidal shape but is well fitted by a stretched exponential curve. This exponential behavior is qualitatively not different from independent molecular relaxation process and its stretched character reveals that the system is not homogeneous. It might be due to the disordered character of the photoinduced phase in relation with two different conformations of one metallocycle of the [Fe(Hpy-DAPP)] cation due to steric constraints.

ACKNOWLEDGMENTS

This work was partly supported by the European Node of Excellence NOE MAGMANet (Contract No. 515767-2), the European FLASH network (Grant No. MRTN-CT-2003-503641), the National Research Agency (ANR "UlTiMATE" Grant No. NT09-3-548342), and the Région Bretagne (PRIR Femtocom 2178). The authors also thank the members of the GDR Magnétisme et Commutation Moléculaire (MCM 2007-2011) for interesting discussions as well as the ONIS platform (University Rennes 1) for the use of the HR800 Raman spectrometer.

*Corresponding author; marylise.buron@univ-rennes1.fr

[1] P. Gütlich, A. Hauser, and H. Spiering, Angew. Chem. **33**, 2024 (1994).
[2] *Spin Crossover in Transition Metal Compounds*, Topics in Current Chemistry, edited by P. Gütlich and H. A. Goodwin (Springer-Verlag, Berlin, New York, 2004), Vol. 233–235.
[3] S. Decurtins, P. Gütlich, C. P. Köhler, H. Spiering, and A. Hauser, Chem. Phys. Lett. **105**, 1 (1984).
[4] H. Spiering, K. Boukheddaden, J. Linares, and F. Varret, Phys. Rev. B **70**, 184106 (2004).
[5] M. Nishino, K. Boukheddaden, Y. Konishi, and S. Miyashita, Phys. Rev. Lett. **98**, 247203 (2007).
[6] S. Miyashita, Y. Konishi, M. Nishino, H. Tokoro, and P. A. Rikvold, Phys. Rev. B **77**, 014105 (2008).
[7] Y. Konishi, H. Tokoro, M. Nishino, and S. Miyashita, Phys. Rev. Lett. **100**, 067206 (2008).
[8] K. Boukheddaden, M. Nishino, and S. Miyashita, Phys. Rev. Lett. **100**, 177206 (2008).
[9] H. Köppen, E. W. Müller, C. P. Köhler, H. Spiering, E. Meissner, and P. Gütlich, Chem. Phys. Lett. **91**, 348 (1982).
[10] D. Chernyshov, M. Hostettler, K. W. Törnroos, and H. B. Bürgi, Angew. Chem., Int. Ed. **42**, 3825 (2003).
[11] N. Huby, L. Guérin, E. Collet, L. Toupet, J. C. Ameline, H. Cailleau, T. Roisnel, T. Tayagaki, and K. Tanaka, Phys. Rev. B **69**, 020101(R) (2004).
[12] G. S. Matouzenko, D. Luneau, G. Molnar, N. Ould Moussa, S. Zein, S. A. Borshch, A. Bousseksou, and F. Averseng, Eur. J. Inorg. Chem. 2006, 2671.
[13] D. Chernyshov, B. Vangdal, K. W. Törnroos, and H.-B. Bürgi, New J. Chem. **33**, 1277 (2009).
[14] T. Tayagaki and K. Tanaka, Phys. Rev. Lett. **86**, 2886 (2001).
[15] T. Tayagaki, K. Tanaka, and H. Okamura, Phys. Rev. B **69**, 064104 (2004).
[16] CRYSALIS RED, Oxford Diffraction Ltd, Version 1.171.32.5, 2007.
[17] A. Altomare, M. C. Burla, M. Camalli, G. Cascareno, C. Giacovazzo, A. Guagliardi, A. G. G. Moliterni, G. Polidori, and R. Spagna, J. Appl. Crystallogr. **32**, 115 (1999).
[18] G. M. Sheldrick, Acta Crystallogr., Sect. A: Found. Crystallogr. **64**, 112 (2008).
[19] CCDC-746481 up to CCDC-746484 contains the supplementary crystallographic data for the structures solved at 290 K, 270 K, 145 K, and 80 K, respectively. CCDC-746514 contains the structure solved at 80 K under light irradiation (658 nm) and CCDC-746589 contains that solved at 80K after the sample quenching. These data can be obtained free of charge via www.ccdc.cam.ac.uk/conts/retrieving.html (or from the Cambridge Crystallographic Data Centre, 12 Union Road, Cambridge CB21EZ, UK; fax: (+44) 1223–336033; or deposit@ccdc.cam.uk).
[20] V. Petrouleas and J. P. Tuchagues, Chem. Phys. Lett. **137**, 21 (1987).
[21] D. Boinnard, A. Bousseksou, A. Dworkin, J. M. Savariault, F. Varret, and J. P. Tuchages, Inorg. Chem. **33**, 271 (1994).
[22] Y. Garcia, O. Kahn, L. Rabardel, B. Chansou, L. Salmon, and J. P. Tuchages, Inorg. Chem. **38**, 4663 (1999).
[23] G. S. Matouzenko, J. F. Létard, S. Lecocq, A. Bousseksou, L. Capes, L. Salmon, M. Perrin, O. Kahn, and A. Collet, Eur. J. Inorg. Chem. 2001, 2935.
[24] W. Hibbs, P. J. Van Koningsbruggen, A. M. Arif, W. W. Shum, and J. S. Miller, Inorg. Chem. **42**, 5645 (2003).
[25] C. Genre, E. Jeanneau, A. Bousseksou, D. Luneau, S. A. Borshch, and G. S. Matouzenko, Chem.-Eur. J. **14**, 697 (2008).
[26] A. Bousseksou, J. Nasser, J. Linares, K. Boukheddaden, and F. Varret, J. Phys. I **2**, 1381 (1992).
[27] A. Bousseksou, F. Varret, and J. Nasser, J. Phys. I **3**, 1463 (1993).
[28] M. Nishino, K. Boukheddaden, S. Miyashita, and F. Varret, Phys. Rev. B **68**, 224402 (2003).
[29] T. Luty and K. Yonemitsu, J. Phys. Soc. Jpn. **73**, 1237 (2004).
[30] D. Chernyshov, H. B. Bürgi, M. Hostettler, and K. W. Törnroos, Phys. Rev. B **70**, 094116 (2004).
[31] J. F. Létard, P. Guionneau, L. Rabardel, J. A. K. Howard, A. E. Goeta, D. Chasseau, and O. Kahn, Inorg. Chem. **37**, 4432 (1998).
[32] J. F. Létard, J. Mater. Chem. **16**, 2550 (2006).
[33] K. Boukheddaden, I. Shteto, B. Hôo, and F. Varret, Phys. Rev. B **62**, 14806 (2000).
[34] A. Hauser, J. Adler, and P. Gütlich, Chem. Phys. Lett. **152**, 468 (1988).
[35] A. Hauser, J. Jeftic, H. Romstedt, R. Hinek, and H. Spiering, Coord. Chem. Rev. **190-192**, 471 (1999).
[36] J. Kusz, P. Gütlich, and H. Spiering, Top. Curr. Chem. **234**, 129 (2004).
[37] P. Guionneau, M. Marchivie, G. Bravic, J. F. Létard, and D. Chasseau, J. Mater. Chem. **12**, 2546 (2002).
[38] M. Marchivie, P. Guionneau, J. F. Létard, and D. Chasseau, Acta Crystallogr., Sect. B: Struct. Sci. **59**, 479 (2003).
[39] J. P. Tuchages, A. Bousseksou, G. Molnar, and J. J. McGarvey, Top. Curr. Chem. **235**, 85 (2004).
[40] D. Chernyshov, N. Klinduhov, K. W. Törnroos, M. Hostettler, B. Vangdal, and H.-B. Bürgi, Phys. Rev. B **76**, 014406 (2007).
[41] S. Bonnet, M. A. Siegler, J. S. Costa, G. Molnar, A. Bousseksou, A. L. Spek, P. Gamez, and J. Reedijk, Chem. Commun. **2008**, 5619 (2008).
[42] N. Bréfuel, H. Watanabe, L. Toupet, J. Come, N. Matsumoto, E. Collet, K. Tanaka, and J.-P. Tuchages, Angew. Chem., Int. Ed. **48**, 9304 (2009).
[43] B. A. Leita, S. M. Neville, G. J. Halder, B. Moubaraki, C. J. Kepert, J. F. Létard, and K. S. Murray, Inorg. Chem. **46**, 8784 (2007).
[44] S. Bonnet, G. Molnar, J. S. Costa, M. A. Siegler, A. L. Spek, A. Bousseksou, W.-T. Fu, P. Gamez, and J. Reedijk, Chem. Mater. **21**, 1123 (2009).